



# The characterization and activity of F-doped vanadia/titania for the selective catalytic reduction of NO with NH<sub>3</sub> at low temperatures

Yuntao Li, Qin Zhong\*

School of Chemical Engineering, Nanjing University of Science and Technology, Nanjing 210094, PR China

## ARTICLE INFO

### Article history:

Received 10 March 2009  
Received in revised form 9 July 2009  
Accepted 13 July 2009  
Available online 17 July 2009

### Keywords:

Low-temperature selective catalytic reduction  
F-doping  
Vanadia/titania  
Superoxide ions

## ABSTRACT

A F-doped vanadia/titania catalyst has been developed by partly substituting the lattice oxygen of the catalyst with fluorine, using NH<sub>4</sub>F as a precursor. The aim of this novel design was to promote the activity of a catalyst with low vanadia loading in the low-temperature selective catalytic reduction of NO with NH<sub>3</sub>. Analysis by N<sub>2</sub> physisorption, XPS, ICP, XRD, ESR and PL spectra showed that fluorine doping facilitated the formation of V<sup>4+</sup> and Ti<sup>3+</sup> ions mainly by charge compensation, promoted the distribution of vanadium on the catalyst surface, and increased the amount of surface superoxide ions. The catalytic activity of NO removal was promoted by F-doping. And the catalyst with [F]/[Ti] = 1.35 × 10<sup>-2</sup> showed the highest NO removal efficiency in SCR reaction at low temperatures.

© 2009 Elsevier B.V. All rights reserved.

## 1. Introduction

Nitrogen oxides (NO<sub>x</sub>) emitted from automobiles and stationary sources are major causes of acid rain as well as photochemical smog through their reactions with hydrocarbons. Selective catalytic reduction (SCR) of NO<sub>x</sub> using NH<sub>3</sub> as a reductant is now widely used for the treatment of waste gases from stationary sources. The commercial catalyst for this deNO<sub>x</sub> process is V<sub>2</sub>O<sub>5</sub>-WO<sub>3</sub> (MoO<sub>3</sub>)/TiO<sub>2</sub> (anatase) with less than 1% V<sub>2</sub>O<sub>5</sub> loading. The high operating temperature of this catalyst, typically 573–673 K, makes it necessary to locate the SCR unit upstream of the precipitator in order to avoid reheating the flue gas. Consequently, the life of the catalyst is shortened because of corrosion and abrasion from the high concentration of ash. When the temperature of the flue gas is above the operating temperature of the catalyst, the catalyst itself can become sintered and deactivated. In addition, the high temperature may cause side reactions, such as oxidation of NH<sub>3</sub> into NO and formation of N<sub>2</sub>O [1]. However, this could be avoided by locating the SCR unit downstream of the precipitator and even downstream of desulfurizer, through the development of a low-temperature (<523 K) SCR. The end results of temperature reduction are an increase in the operational lifetime of the catalyst relative to existing configurations, as well as a lowering of investment costs.

The core of low-temperature SCR technology is the existence of a catalyst that is suitable for low-temperature flue gas conditions. For presently available vanadia/titania catalysts, performance of low-temperature SCR could be promoted by increasing the vanadia loading [1–4]. However, this has the shortcoming of decreasing the selectivity and lifetime of the catalyst as it facilitates SO<sub>2</sub> oxidation [5] and N<sub>2</sub>O formation [2]. Recently, efforts have been made to promote low-temperature SCR performance of vanadia catalysts through the use of promoters such as 1%CrO<sub>3</sub>-6%V<sub>2</sub>O<sub>5</sub>/TiO<sub>2</sub> [3] and 1%MO<sub>x</sub> (M=Fe, Mn, Cu or Cr)-3%V<sub>2</sub>O<sub>5</sub>/mesoporous carbon-coated monoliths [6]. Other approaches have changed the support to materials such as 3-8%V<sub>2</sub>O<sub>5</sub>/carbon-coated monoliths [7–9], 1-7%V<sub>2</sub>O<sub>5</sub>/activated carbon fibers [10], 2.35%V<sub>2</sub>O<sub>5</sub>/carbon nanotubes [11], 1.7%V<sub>2</sub>O<sub>5</sub>/WO<sub>x</sub> or SO<sub>4</sub><sup>2-</sup>/ZrO<sub>2</sub> [12], 8%V<sub>2</sub>O<sub>5</sub>/TiO<sub>2</sub>-SiO<sub>2</sub>-MoO<sub>3</sub> [13], 3-7%VO<sub>x</sub> (x<2.5)/TiO<sub>2</sub> (supports obtained from different companies) [14]. However, these catalysts were unable to reduce the vanadia loading.

The aim of this study was to approach the problem from a different angle, by targeting the non-metal part of the catalyst. We describe a novel F-doped vanadia/titania catalyst formed by partly substituting the lattice oxygen of the catalyst with fluorine. In previous applications, F-doped and fluorinated TiO<sub>2</sub> has been used as a photocatalyst under visible light irradiation [15–20]. However, it has not previously been used as a support for a vanadia catalyst. Narayana et al. [21] revealed that the V<sup>4+</sup> species increased with an increase in V<sub>2</sub>O<sub>5</sub> loading over V<sub>2</sub>O<sub>5</sub>/AlF<sub>3</sub>. Scheurell et al. [22–24], studying the selective oxidative dehydrogenation of propane (ODH), found that VO<sub>x</sub> doped onto AlF<sub>3</sub> showed better redox ability of active vanadium species and more acid sites than

\* Corresponding author. Tel.: +86 25 84315517; fax: +86 25 84315517.  
E-mail addresses: [zq304@mail.njust.edu.cn](mailto:zq304@mail.njust.edu.cn), [zq304@tom.com](mailto:zq304@tom.com) (Q. Zhong).

did  $\text{VO}_x$  doped onto  $\text{Al}_2\text{O}_3$ . However, to the best of our knowledge, F-doped vanadia/titania catalysts for low-temperature SCR of NO with ammonia have not yet been studied.

The present study focuses on the structural and surface properties of a new catalyst formed by fluorine doping, which was characterized by  $\text{N}_2$  physisorption, XPS, ICP, XRD, ESR and PL spectra. We also investigated the SCR activity of the catalyst at low temperatures, as well as the activity when  $\text{H}_2\text{O}$  and  $\text{SO}_2$  existing. This information would contribute to a better understanding of the low-temperature SCR processes over a vanadia/titania catalyst.

## 2. Experimental

### 2.1. Catalyst preparation

The F-doped vanadia/titania catalyst was prepared by a sol-gel method for F-doped titania preparation, followed by impregnation for vanadia loading. The detailed procedure for F-doped titania preparation has been described elsewhere [15], specifically as follows:  $\text{Ti}(\text{OC}_4\text{H}_9)_4$  (0.064 mol) was stabilized by adding 0.128 mol acetylacetone. A color change of the solution from pale yellow to orange occurred under continuous stirring. The solution was diluted with 50 mL of  $\text{NH}_4\text{F}$  ethanolic solutions [15]. After stirring for 2 h at room temperature, the sol was concentrated in a 333 K water bath and subsequently dried at 393 K for 6 h. The gel was calcined at 773 K for 3 h in air, and then sieved (0.701–0.833 mm). After impregnation in ammonium metavanadate solution (plus  $\text{HNO}_3$  at pH 1) [25] in a 333 K water bath and refluxing for 4 h, the sieved titania was dried at 393 K for 6 h and subsequently calcined at 623 K for 4 h. Finally, the F-doped vanadia/titania catalyst was obtained. In the present study, the catalyst and the carrier were denoted as  $\text{VTiF } x$  and  $\text{TiF } x$ , respectively. For example,  $\text{VTiF } 1.35$  meant the catalyst with fluorine content calculated as  $[\text{F}]/[\text{Ti}] = 1.35 \times 10^{-2}$ , and  $\text{TiF } 1.35$  meant the carrier with the same fluorine content.

### 2.2. Catalyst characterization

The  $S_{\text{BET}}$  measurement was carried out in a Micrometrics ASAP 2000 apparatus at 77 K, using  $\text{N}_2$  as the adsorption gas. X-ray photoelectron spectroscopy (XPS) measurements were performed using an ESCALB MK-II with Mg  $K\alpha$  source, calibrated by the C 1s peak at 284.6 eV with an accuracy of  $\pm 0.2$  eV. The approximate content of vanadium was determined by inductively coupled plasma (ICP) spectroscopy (Thermo Electron; Model IRIS Intrepid II XDL). The electron spin resonance (ESR) measurements were made at room temperature using a Bruker EMX-10/12-type spectrometer in the X-band. The photoluminescence (PL) spectra were conducted at room temperature using a Labram-HR800-type spectrophotometer (Jobin Yvon Co., France) with a He–Cd laser ( $\lambda = 325$  nm) as the light source. The X-ray diffraction (XRD) analysis was obtained by a XD-3 diffractometer (Beijing Purkinje General Instrument Co., Ltd, China).

### 2.3. Activity tests

Catalytic activity tests of NO reduced by  $\text{NH}_3$  were carried out at 393–513 K in a fixed-bed flow reactor (i.d. 6.8 mm) under atmospheric pressure. The gas flow was controlled by mass flow meters. The reaction temperature was measured by a K type thermocouple inserted directly into the catalyst bed. The used mass of the catalyst was 0.8000 g with quartz sand as inert. A reaction mixture containing 500 ppm NO + 600 ppm  $\text{NH}_3$  + 5 vol.%  $\text{O}_2$  + 600 ppm  $\text{SO}_2$  (when used) + 2% or 4%  $\text{H}_2\text{O}$  (when used) balanced with  $\text{N}_2$  at a flow rate of  $150 \text{ mL min}^{-1}$  was used, corresponding to a gas hour space velocity (GHSV) of  $14,580 \text{ h}^{-1}$ . Prior to the reaction, the catalyst sample was pre-adsorbed by the reaction mixture, to avoid a decrease of

NO caused by adsorption on the catalyst. Analysis of reactants and products was carried out after a steady reaction of more than 1 h at each testing point. Concentrations of NO and  $\text{SO}_2$  were analyzed by a MRU VARIO PLUS flue gas analyzer (Germany) after passing through concentrated phosphoric acid to avoid the influence of  $\text{NH}_3$  on NO analysis. The  $\text{N}_2\text{O}$  was monitored by a Gasetm Dx-4000 FT-IR gas analyzer (Germany). The selectivity to  $\text{N}_2$  is defined as  $\text{N}_2$  divided by  $(\text{N}_2 + \text{N}_2\text{O})$  on a N-atom basis. The NO conversion is defined as:

$$X = \frac{\text{NO}_{\text{in}} - \text{NO}_{\text{out}}}{\text{NO}_{\text{in}}} \quad (1)$$

The NO reaction rate was expressed by means of the following equation:

$$r = kP_{\text{NO}} \quad (2)$$

for which first order in NO partial pressure and zero order in  $\text{NH}_3$  partial pressure was assumed. In order to compare the activities of different vanadium-loading catalysts, the rate constants  $k_m$  could be evaluated as follows:

$$k_m = -\frac{F_{\text{NO}}^0 \ln(1 - X)/w_m}{P_{\text{NO}}^0} \quad (3)$$

where  $P_{\text{NO}}^0$  is the NO partial pressure,  $F_{\text{NO}}^0$  is the inlet NO molar flux, and  $w_m$  is the vanadium mass [26].

## 3. Results and discussion

### 3.1. Characterization of the F-doped catalysts

#### 3.1.1. Valences of titanium and vanadium

Lee et al. [14] revealed that the participation of lattice oxygen in the reduction of nitrogen oxide and the re-oxidation of gaseous oxygen into lattice oxygen were closely related to the electrons generated due to the valence change of vanadium. They suggested that the non-stoichiometric vanadium oxide produced on the catalyst could activate the electron transfer, thus improving the reduction and/or re-oxidation properties of the catalyst. For a F-doped vanadia/titania catalyst, considering the difference between fluorine and oxygen, we expected that the valences of titanium and vanadium would be influenced by fluorine doping. This was confirmed by the ESR and XPS characterizations of the samples.

The amounts of  $\text{Ti}^{3+}$  and  $\text{V}^{4+}$  ions present in both surface and bulk samples have been examined by ESR at room temperature (as shown in Fig. 1). Since the amount of vanadium loaded onto the catalyst was low (as shown in Table 1), the spectrum of the  $\text{V}^{4+}$  ion was not well-resolved. The spectra of F-doped samples showed a strong

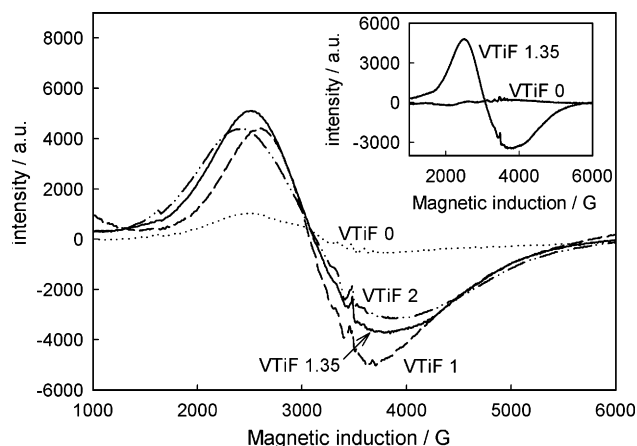


Fig. 1. ESR spectra of the catalysts at room temperature. Insert: ESR spectra of  $\text{VTiF } 0$  and  $\text{VTiF } 1.35$  after subtracting the ESR spectra of their supports, respectively.

**Table 1**  
Vanadia content, BET specific area and the kinetic constants of the catalysts.

	V <sub>2</sub> O <sub>5</sub> (wt.%)	S <sub>BET</sub> (m <sup>2</sup> g <sup>-1</sup> )	k <sub>m</sub> (483 K) (×10 <sup>-9</sup> mol NO(gV) <sup>-1</sup> Pa <sup>-1</sup> s <sup>-1</sup> )	k <sub>m</sub> (513 K) (×10 <sup>-9</sup> mol NO(gV) <sup>-1</sup> Pa <sup>-1</sup> s <sup>-1</sup> )
VTiF 0	0.8	28.77	0.96	2.17
VTiF 1	1.2	20.93	10.51	15.64
VTiF 1.35	0.8	23.55	11.36	43.02
VTiF 2	0.9	27.66	4.81	9.84

and broad peak, related to the Ti<sup>3+</sup> ion, which significantly reduced the spectral resolution of V<sup>4+</sup> ion. Through an integral of this strong and broad peak, we could obtain that the peak area decreased as following order: VTiF 1.35 > VTiF 1 > VTiF 2 > VTiF 0. Within the detection depth of XPS, It shows that the binding energies of Ti 2p<sub>3/2</sub>, V 2p<sub>3/2</sub>, and O 1s of VTiF 1.35 shifted by 0.3, 0.35, and 0.45 eV, respectively, toward the low binding energy direction (as shown in Fig. 2), when compared with those of VTiF 0. Thus, there was a decrease in electrons both lost by Ti and V and gained by O, indicating that the valence states of Ti and V were not entirely +4 and +5, respectively. However, the F 1s was not observed, due to the low F-doping content (more details about the fluorine content in VTiF 1.35 evaluated from XPS are shown in the Supporting Information). The chemical states were analyzed in detail by deconvolution using Lorentzian–Gaussian mixture peak fitting. The deconvoluted XPS spectra (not shown) showed that the Ti<sup>3+</sup>/Ti<sup>4+</sup> ratios were 0.57 and 1.22 for VTiF 0 and VTiF 1.35, respectively. The V<sup>4+</sup>/V<sup>5+</sup> ratios were 0.79 and 1.19 for VTiF 0 and VTiF 1.35, respectively. The presence of V<sup>4+</sup> was related to the condition of vanadia impregnation [25] and was promoted by F-doping. From the ESR and XPS characterizations, we can conclude that the samples in this study contained mixed valences of Ti and V, and that the amounts of V<sup>4+</sup> and Ti<sup>3+</sup> ions were promoted by F-doping. This indicated an improvement in the reduction and/or re-oxidation properties of the catalyst [21–24].

By subtracting the corresponding support spectrum (as shown in the insert of Fig. 1), the Ti<sup>3+</sup> ion of the VTiF 0 sample was completely formed at the support preparation stage. In contrast, the Ti<sup>3+</sup> ion of the F-doped sample VTiF 1.35 was formed primarily at the vanadium loading stage. Previous studies [27,28] have revealed that V<sup>4+</sup> ions could be included as dopants inside a TiO<sub>2</sub> matrix, leading formally to a V<sub>x</sub>Ti<sub>1-x</sub>O<sub>2</sub> solid solution. The cationic vacancies formed by Ti<sup>3+</sup> moving to interstitial sites were considered to be the prerequisites for the introduction of V<sup>4+</sup> ions into the TiO<sub>2</sub> matrix. Since Ti<sup>3+</sup> ions were produced during heat-treatment due to the decomposition of organic compounds, the existence of Ti<sup>3+</sup> and V<sup>4+</sup> ions could be inferred. However, the amount of Ti<sup>3+</sup> ion in the F-doped sample increased after vanadium loading, which indicated the existence of another process for the formation of V<sup>4+</sup> ion in addition to the formation of V<sub>x</sub>Ti<sub>1-x</sub>O<sub>2</sub>. Therefore, it is reasonable to propose that there might be a charge compensation process [29,30] between vanadium and titanium, as in the following equations:

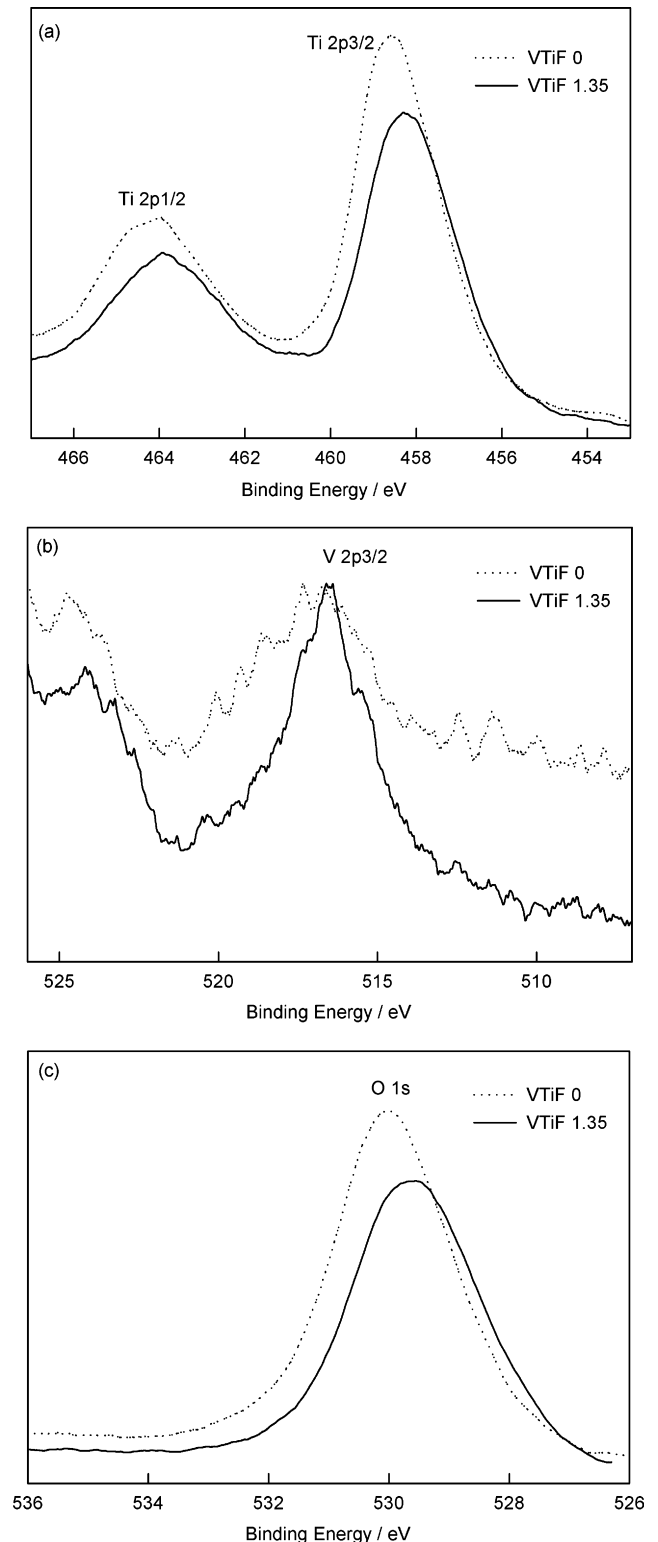
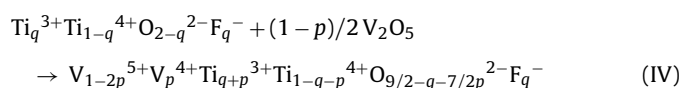
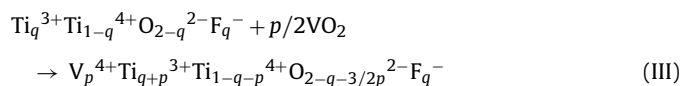
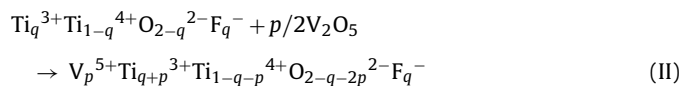
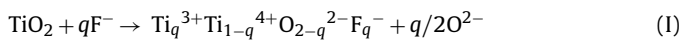


**Fig. 2.** XPS spectra of VTiF 0 and VTiF 1.35 catalysts: (a) Ti, (b) V, and (c) O.

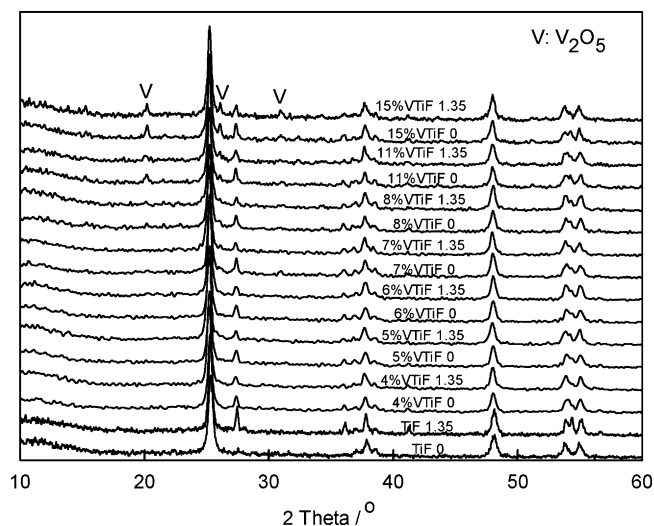
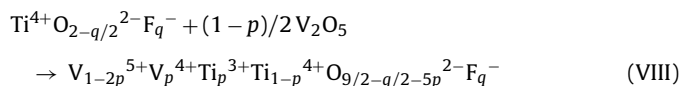
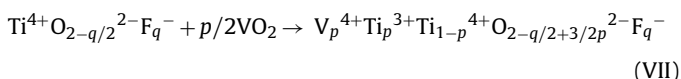
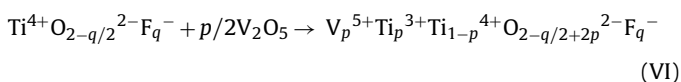
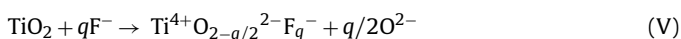


Fig. 3. X-ray diffraction patterns for 4–15 wt.%  $V_2O_5$  content catalysts supported both on F-doped and undoped titania.

or



### 3.1.2. Distribution of vanadium

Vanadium, as an active component, is the adsorption site for ammonia in the low-temperature SCR process [31]. Hence, promoting the distribution of vanadium increases the amount of effective vanadium that can participate in a low-temperature SCR reaction, which in turn facilitates the reaction. Within the detection depth of XPS, the F-doped sample VTiF 1.35 appeared to present more vanadium atoms (0.57%) than did the undoped sample VTiF 0 (0.21%). Moreover, to compare the distribution of vanadium over F-doped titania and undoped titania, we prepared 4–15 wt.%  $V_2O_5$  content catalysts supported on TiF 1.35 and TiF 0. The samples were characterized by XRD (as shown in Fig. 3). When the  $V_2O_5$  content was below 7%, it did not detect  $V_2O_5$  for both F-doped and undoped samples. However, when the  $V_2O_5$  content was 8%, the peak of  $V_2O_5$  appeared (pdf 41-1426) for both samples. The difference of XRD patterns between the F-doped and undoped sample was that the peak of  $V_2O_5$  over F-doped sample was weaker than that over undoped sample. This difference existed even when the  $V_2O_5$  content was up to 15%. Therefore, F-doping could make vanadia well-dispersed over the support.

### 3.1.3. Surface superoxide ions

For commercialized SCR processes at temperatures between 573 and 673 K, it is agreed that the reaction mechanism involves the interaction of adsorbed ammonia ( $NH_4^+$ ) with gaseous NO [31]. However, for SCR process at low temperatures, increasingly more studies [32–35] are revealing that reactive  $NO_y$  (nitro and nitrate) groups are the intermediates that react with adsorbed ammonia (most probably adsorbed onto Lewis acid sites [1,36–38]). Thus, the

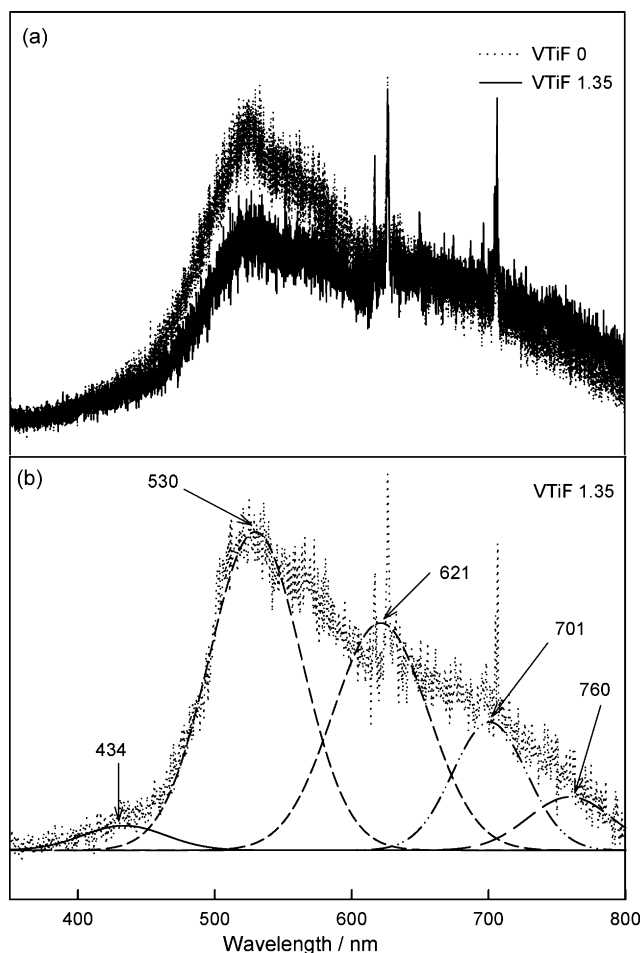


Fig. 4. PL spectra of VTiF 0 and VTiF 1.35 catalysts (a) and deconvolution of PL spectra of VTiF 1.35 (b) using Lorentzian–Gaussian peak fitting.

formation of  $NO_y$  from gaseous NO is the key process. Wang et al. [39] have proposed that the  $NO_y$  groups are formed from NO and an adsorbed superoxide ion. This important role of superoxide ions in the low-temperature SCR process has been confirmed by other studies [40,41]. Therefore, we also investigated the superoxide ion content on the catalyst surface.

Superoxide ions could be formed by oxygen adsorption onto the surface color centers at low temperature [42]. These color centers or F centers could be characterized by photoluminescence (PL) spectra. Fig. 4 shows the PL spectra of VTiF 0 and VTiF 1.35 samples, from which we can observe color centers with one trapped electron at 530 nm [16,17] (more details are shown in Fig. S1 of the Supporting Information). Luminescence could be quenched by adsorption of oxygen [42], therefore the peak intensity at 530 nm of the F-doped sample was lower than that of the undoped one, which may represent a different adsorption capability for oxygen. In other words, a F-doped sample could adsorb more oxygen than an undoped sample. This was confirmed by ESR spectra of superoxide ions ( $g_{yy} = 2.0047$  [42,43] as shown in Fig. 5). In overview, F-doping increased the amount of superoxide ions and the affinity for oxygen. Among the samples involved in the present study, VTiF 1.35 showed the most amount of superoxide ions, and then decreased as: VTiF 1 > VTiF 2 > VTiF 0. As the formation of superoxide ion over  $V^{4+}$  lead to the formation of  $V^{5+}-O_2^-$ , it also makes the decrease of the spectral resolution of  $V^{4+}$  ion, which has been discussed in Section 3.1.1. From the intensities of  $g_{yy}$  over VTiF 0, VTiF 1.35 and their carriers in Fig. 5, we can determine that the vanadia loading could facilitate the formation of superoxide ions.



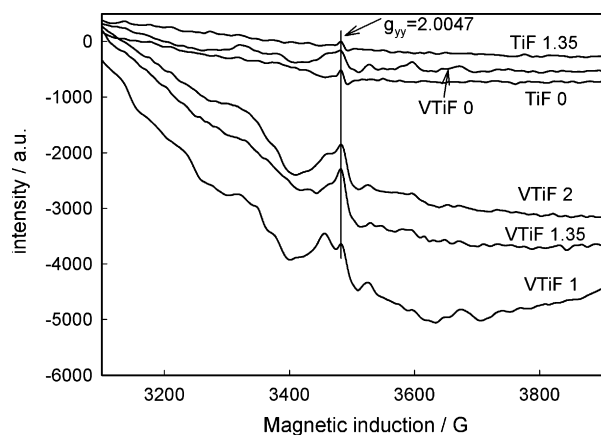


Fig. 5. ESR spectra of superoxide ions over the catalysts.

### 3.2. Low-temperature SCR activity of the catalysts

The NO removal efficiency of the catalysts at 483 and 513 K was shown in Table 1. It indicated that the rate constants of the catalysts were significantly increased by F-doping. The evolution of rate constants followed as: VTiF 1.35 > VTiF 1 > VTiF 2 > VTiF 0. Comparing the rate constants with those in Ref. [26], it can be seen that the catalysts developed in this work have a lower rate constant than the previously reported. This could be due to a lower specific surface area derived from the preparation method employed (as shown in Table 1). The formation of  $N_2O$  was <3 ppm for all the samples under our testing conditions, and thus the selectivity to  $N_2$  was promising.

Moreover, we conducted a  $SO_2$  and  $H_2O$  resistance experiment for the catalyst. This type of study is essential for initiating the practical use of vanadia/titania catalysts for  $NO_x$  removal with  $NH_3$ . Previous studies [44,45] have revealed that adding  $SO_2$  could increase the activity of a vanadia catalyst, but  $H_2O$  could not. Moisture inhibited the SCR reaction of a vanadia catalyst, but this inhibition was reversible and decreased with increasing reaction temperature [10,36]. Fig. 6 shows the evolution of NO conversion and  $SO_2$  concentration for a VTiF 1.35 sample with time on stream at 483 and 513 K. Adding  $SO_2$  had almost no influence on NO conversion at 483 and 513 K, for the NO conversions were very high at both temperatures. However, adding  $H_2O$  without  $SO_2$  inhibited the reaction and further deterioration was seen as the moisture content was increased (Fig. 6(b), point “C”). When both  $H_2O$  and  $SO_2$  were added, the inhibition was more severe than the sum of inhibitions

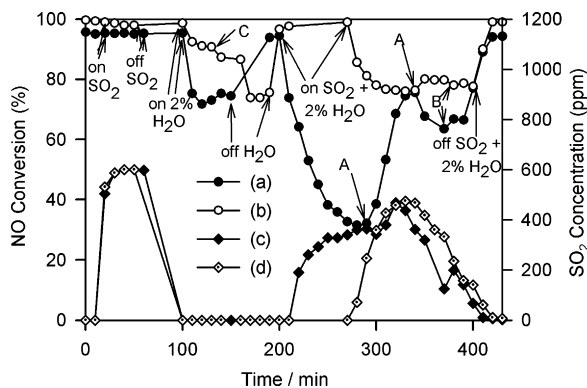


Fig. 6. The evolution of NO conversion and  $SO_2$  concentration over VTiF 1.35 with time on stream at 483 and 513 K: (a) NO conversion at 483 K, (b) NO conversion at 513 K, (c)  $SO_2$  concentration at 483 K, and (d)  $SO_2$  concentration at 513 K. Point “A”: changing ammonia concentration from 600 to 900 ppm, point “B”: changing ammonia concentration from 900 to 1200 ppm, and point “C”: changing water content from 2% to 4%.

observed when  $H_2O$  and  $SO_2$  were added individually, indicating a synergistic inhibitory effect of  $H_2O$  and  $SO_2$ . However, this synergistic inhibition was alleviated, although not completely eradicated, by increasing the concentration of ammonia from 600 to 900 ppm (even to 1200 ppm, as shown in Fig. 6, point “A” and “B”). This suggested a competition for  $NH_3$  between NO and  $SO_2$ , which could be seen when the evolution of NO removal efficiency and  $SO_2$  concentration were compared (Fig. 6), and which was consistent with a previous study by Kasaoka et al. [46]. The above inhibitions could be reduced by increasing reaction temperature and were reversible, again in agreement with previous studies [10,36].

## 4. Conclusions

To improve the NO removal efficiency of low-vanadium-loading catalysts for low-temperature SCR, a novel fluorine doped vanadia/titania catalyst has been developed. In this catalyst, the lattice oxygen was partially substituted with fluorine using  $NH_4F$  as a precursor. In the present work, we characterized this catalyst and tested its catalytic activity in low-temperature SCR. When the valences of titanium and vanadium, the distribution of vanadium, and the surface superoxide ions of both the F-doped and undoped catalysts were examined, F-doping was found to facilitate the formation of  $V^{4+}$  and  $Ti^{3+}$  ions, to promote the distribution of vanadium on the catalyst surface, and to increase the amount of surface superoxide ions. The catalytic activity of NO removal was promoted by F-doping. In our study, The catalyst with  $[F]/[Ti] = 1.35 \times 10^{-2}$  showed the highest rate constant in low-temperature SCR reaction. Although the changes in the catalyst caused after by F-doping were related to the improvement of NO removal efficiency, it still needs more in situ work to investigate the structure–activity relationships over this new catalyst. The further work is carrying out in our lab.

## Acknowledgements

We sincerely appreciate the help from Dr. Liang Chen with respect to the  $N_2O$  measurements in the Tsinghua University, China. Support from the National High Technology Research and Development Program of China (Grant No. 2007AA0618025) and the Jiangsu Natural Science Foundation of China (Grant No. BK2007215 and Grant No. BK2008421) are gratefully acknowledged.

## Appendix A. Supplementary data

Supplementary data associated with this article can be found, in the online version, at doi:10.1016/j.jhazmat.2009.07.039.

## References

- [1] D.A. Peña, B.S. Uphade, P.G. Smirniotis,  $TiO_2$ -supported metal oxide catalysts for low-temperature selective catalytic reduction of NO with  $NH_3$ . I. Evaluation and characterization of first row transition metals, *J. Catal.* 221 (2004) 421–431.
- [2] J.A. Martín, M. Yates, P. Ávila, S. Suárez, J. Blanco, Nitrous oxide formation in low temperature selective catalytic reduction of nitrogen oxides with  $V_2O_5/TiO_2$  catalysts, *Appl. Catal. B* 70 (2007) 330–334.
- [3] I. Giakoumelou, Ch. Fountzoula, Ch. Kordulis, S. Boghosian, NO reduction with  $NH_3$  over chromia–vanadia catalysts supported on  $TiO_2$ : an in situ Raman spectroscopic study, *Catal. Today* 73 (2002) 255–262.
- [4] Z. Zhu, Z. Liu, S. Liu, H. Niu, A novel carbon-supported vanadium oxide catalyst for NO reduction with  $NH_3$  at low temperatures, *Appl. Catal. B* 23 (1999) L229–L233.
- [5] H. Kamata, H. Ohara, K. Takahashi, A. Yukimura, Y. Seo,  $SO_2$  oxidation over the  $V_2O_5/TiO_2$  SCR catalyst, *Catal. Lett.* 73 (2001) 79–83.
- [6] E. García-Bordejé, A. Monzón, M.J. Lázaro, R. Moliner, Promotion by a second metal or  $SO_2$  over vanadium supported on mesoporous carbon-coated monoliths for the SCR of NO at low temperature, *Catal. Today* 102–103 (2005) 177–182.
- [7] E. García-Bordejé, L. Calvillo, M.J. Lázaro, R. Moliner, Vanadium supported on carbon-coated monoliths for the SCR of NO at low temperature: effect of pore structure, *Appl. Catal. B* 50 (2004) 235–242.

- [8] E. García-Bordejé, J.L. Pinilla, M.J. Lázaro, R. Moliner,  $\text{NH}_3$ -SCR of NO at low temperatures over sulphated vanadia on carbon-coated monoliths: effect of  $\text{H}_2\text{O}$  and  $\text{SO}_2$  traces in the gas feed, *Appl. Catal. B* 66 (2006) 281–287.
- [9] E. García-Bordejé, J.L. Pinilla, M.J. Lázaro, R. Moliner, J.L.G. Fierro, Role of sulphates on the mechanism of  $\text{NH}_3$ -SCR of NO at low temperatures over presulphated vanadium supported on carbon-coated monoliths, *J. Catal.* 233 (2005) 166–175.
- [10] G. Marbán, R. Antuña, A.B. Fuertes, Low-temperature SCR of  $\text{NO}_x$  with  $\text{NH}_3$  over activated carbon fiber composite-supported metal oxides, *Appl. Catal. B* 41 (2003) 323–338.
- [11] B.C. Huang, R. Huang, D.J. Jin, D.Q. Ye, Low temperature SCR of NO with  $\text{NH}_3$  over carbon nanotubes supported vanadium oxides, *Catal. Today* 126 (2007) 279–283.
- [12] J. Due-Hansen, S. Boghosian, A. Kustov, P. Frstrup, G. Tsilomelekis, K. Ståhl, C.H. Christensen, R. Fehrmann, Vanadia-based SCR catalysts supported on tungstated and sulfated zirconia: influence of doping with potassium, *J. Catal.* 251 (2007) 459–473.
- [13] M. Kobayashi, R. Kuma, A. Morita, Low temperature selective catalytic reduction of NO by  $\text{NH}_3$  over  $\text{V}_2\text{O}_5$  supported on  $\text{TiO}_2$ - $\text{SiO}_2$ - $\text{MoO}_3$ , *Catal. Lett.* 112 (2006) 37–44.
- [14] J.Y. Lee, S.H. Hong, S.P. Cho, S.C. Hong, The study of  $\text{deNO}_x$  catalyst in low temperature using nano-sized supports, *Curr. Appl. Phys.* 6 (2006) 996–1001.
- [15] A. Hattori, M. Yamamoto, H. Tada, S. Ito, A promoting effect of  $\text{NH}_4\text{F}$  addition on the photocatalytic activity of sol-gel  $\text{TiO}_2$  films, *Chem. Lett.* 27 (1998) 707–708.
- [16] D. Li, H. Haneda, S. Hishita, N. Ohashi, N.K. Labhsetwar, Fluorine-doped  $\text{TiO}_2$  powders prepared by spray pyrolysis and their improved photocatalytic activity for decomposition of gas-phase acetaldehyde, *J. Fluorine Chem.* 126 (2005) 69–77.
- [17] D. Li, H. Haneda, N.K. Labhsetwar, S. Hishita, N. Ohashi, Visible-light-driven photocatalysis on fluorine-doped  $\text{TiO}_2$  powders by the creation of surface oxygen vacancies, *Chem. Phys. Lett.* 401 (2005) 579–584.
- [18] H.F. Jiang, H.Y. Song, Z.X. Zhou, X.Q. Liu, G.Y. Meng, The roles of  $\text{Li}^+$  and  $\text{F}^-$  ions in Li-F-codoped  $\text{TiO}_2$  system, *J. Phys. Chem. Solids* 68 (2007) 1830–1835.
- [19] Q. Wang, C.C. Chen, D. Zhao, W.H. Ma, J.C. Zhao, Change of adsorption modes of dyes on fluorinated  $\text{TiO}_2$  and its effect on photocatalytic degradation of dyes under visible irradiation, *Langmuir* 24 (2008) 7338–7345.
- [20] N. Todorova, T. Giannakopoulou, T. Vaimakis, C. Trapalis, Structure tailoring of fluorine-doped  $\text{TiO}_2$  nanostructured powders, *Mater. Sci. Eng. B* 152 (2008) 50–54.
- [21] K.V. Narayana, B.D. Raju, S.K. Masthan, V.V. Rao, P.K. Rao, R. Subrahmanian, A. Martin, ESR spectroscopic characterization of  $\text{V}_2\text{O}_5/\text{AlF}_3$  ammoxidation catalysts, *Catal. Commun.* 5 (2004) 457–462.
- [22] K. Scheurell, E. Kemnitz, Amorphous aluminium fluoride as new matrix for vanadium-containing catalysts, *J. Mater. Chem.* 15 (2005) 4845–4853.
- [23] K. Scheurell, G. Scholz, E. Kemnitz, Structural study of  $\text{VO}_x$  doped aluminium fluoride and aluminium oxide catalysts, *J. Solid State Chem.* 180 (2007) 749–758.
- [24] K. Scheurell, G. Scholz, A. Pawlik, E. Kemnitz,  $\text{VO}_x$  doped  $\text{Al}_2\text{O}_3$  and  $\text{AlF}_3$ —a comparison of bulk, surface and catalytic properties, *Solid State Sci.* 10 (2008) 873–883.
- [25] F. Chiker, J.Ph. Nogier, J.L. Bonardet, Sub-monolayer  $\text{V}_2\text{O}_5$ -anatase  $\text{TiO}_2$  and Eurocat catalysts: IR, Raman and XPS characterisation of  $\text{VO}_x$  dispersion, *Catal. Today* 78 (2003) 139–147.
- [26] T. Valdés-Solís, G. Marbán, A.B. Fuertes, Low-temperature SCR of  $\text{NO}_x$  with  $\text{NH}_3$  over carbon-ceramic supported catalysts, *Appl. Catal. B* 46 (2003) 261–271.
- [27] A. Davidson, M. Che, Temperature-induced diffusion of probe vanadium(IV) ions into the matrix of titanium dioxide as investigated by ESR techniques, *J. Phys. Chem.* 96 (1992) 9909–9915.
- [28] D.E. Gu, B.C. Yang, Y.D. Hu, A novel method for preparing V-doped titanium dioxide thin film photocatalysts with high photocatalytic activity under visible light irradiation, *Catal. Lett.* 118 (2007) 254–259.
- [29] J.C. Yu, J.G. Yu, W.K. Ho, Z.T. Jiang, L.Z. Zhang, Effects of F-doping on the photocatalytic activity and microstructures of nanocrystalline  $\text{TiO}_2$  powders, *Chem. Mater.* 14 (2002) 3808–3816.
- [30] H. Lin, S. Kumon, H. Kozuka, T. Yoko, Electrical properties of sol-gel-derived transparent titania films doped with ruthenium and tantalum, *Thin Solid Films* 315 (1998) 266–272.
- [31] G. Busca, L. Lietti, G. Ramisa, F. Berti, Chemical and mechanistic aspects of the selective catalytic reduction of  $\text{NO}_x$  by ammonia over oxide catalysts: a review, *Appl. Catal. B* 18 (1998) 1–36.
- [32] W.S. Kijlstra, D.S. Brands, E.K. Poels, A. Blik, Mechanism of the selective catalytic reduction of NO by  $\text{NH}_3$  over  $\text{MnO}_x/\text{Al}_2\text{O}_3$ , *J. Catal.* 171 (1997) 208–218.
- [33] M. Koebel, M. Elsener, G. Madia, Reaction pathways in the selective catalytic reduction process with NO and  $\text{NO}_2$  at low temperatures, *Ind. Eng. Chem. Res.* 40 (2001) 52–59.
- [34] C. Ciardelli, I. Nova, E. Tronconi, D. Chatterjee, B. Bandl-Konrad, A nitrate route for the low temperature fast SCR reaction over a  $\text{V}_2\text{O}_5$ - $\text{WO}_3/\text{TiO}_2$  commercial catalyst, *Chem. Commun.* (2004) 2718–2719.
- [35] A. Grossale, I. Nova, E. Tronconi, D. Chatterjee, M. Weibel, The chemistry of the  $\text{NO}/\text{NO}_2$ - $\text{NH}_3$  “fast” SCR reaction over Fe-ZSM5 investigated by transient reaction analysis, *J. Catal.* 256 (2008) 312–322.
- [36] Z.G. Huang, Z.Y. Liu, X.L. Zhang, Q.Y. Liu, Inhibition effect of  $\text{H}_2\text{O}$  on  $\text{V}_2\text{O}_5/\text{AC}$  catalyst for catalytic reduction of NO with  $\text{NH}_3$  at low temperature, *Appl. Catal. B* 63 (2006) 260–265.
- [37] Z.B. Wu, B.Q. Jiang, Y. Liu, H.Q. Wang, R.B. Jin, DRIFT study of manganese/titania-based catalysts for low-temperature selective catalytic reduction of NO with  $\text{NH}_3$ , *Environ. Sci. Technol.* 41 (2007) 5812–5817.
- [38] P.G. Smirniotis, D.A. Peña, B.S. Uphade, Low-temperature selective catalytic reduction (SCR) of NO with  $\text{NH}_3$  by using Mn, Cr, and Cu oxides supported on hombikat  $\text{TiO}_2$ , *Angew. Chem. Int. Ed.* 40 (2001) 2479–2482.
- [39] X. Wang, H.Y. Chen, W.M.H. Sachtler, Mechanism of the selective reduction of  $\text{NO}_x$  over Co/MFI: comparison with Fe/MFI, *J. Catal.* 197 (2001) 281–291.
- [40] G.S. Szymański, T. Grzybek, H. Papp, Influence of nitrogen surface functionalities on the catalytic activity of activated carbon in low temperature SCR of  $\text{NO}_x$  with  $\text{NH}_3$ , *Catal. Today* 90 (2004) 51–59.
- [41] R. Brosius, J.A. Martens, Reaction mechanisms of lean-burn hydrocarbon SCR over zeolite catalysts, *Top. Catal.* 28 (2004) 119–130.
- [42] M. Anpo, M. Che, B. Fubini, E. Garrone, E. Giamello, M.C. Paganini, Generation of superoxide ions at oxide surfaces, *Top. Catal.* 8 (1999) 189–198.
- [43] E. Giamello, Reactive intermediates formed upon electron transfer from the surface of oxide catalysts to adsorbed molecules, *Catal. Today* 41 (1998) 239–249.
- [44] I. Giakoumelou, C. Fountzoula, C. Kordulis, S. Boghosian, Molecular structure and catalytic activity of  $\text{V}_2\text{O}_5/\text{TiO}_2$  catalysts for the SCR of NO by  $\text{NH}_3$ : in situ Raman spectra in the presence of  $\text{O}_2$ ,  $\text{NH}_3$ , NO,  $\text{H}_2$ ,  $\text{H}_2\text{O}$ , and  $\text{SO}_2$ , *J. Catal.* 239 (2006) 1–12.
- [45] M.D. Amiridis, I.E. Wachs, G. Deo, J.-M. Jehng, D.S. Kim, Reactivity of  $\text{V}_2\text{O}_5$  catalysts for the selective catalytic reduction of NO by  $\text{NH}_3$ : influence of vanadia loading,  $\text{H}_2\text{O}$ , and  $\text{SO}_2$ , *J. Catal.* 161 (1996) 247–253.
- [46] S. Kasaoka, E. Sasaoka, H. Iwasaki, Vanadium oxides ( $\text{V}_2\text{O}_x$ ) catalysts for dry-type and simultaneous removal of sulfur oxides and nitrogen oxides with ammonia at low temperature, *Bull. Chem. Soc. Jpn.* 62 (1989) 1226–1232.